Carbohydrate Polymers 8 (1988) 271–284

Xanthan/Carob Interactions at Very Low Concentration

G. Cuvelier & B. Launay

Food Science Department, ENSIA, 1. av. des Olympiades,
91305 Massy, France

(Received 31 July 1987; revised version received 10 October 1987;
accepted 11 January 1988)

ABSTRACT

Xanthan/carob interactions at very low concentration have been studied by viscosity measurements at 25°C and in 0·1 M *NaCl. The existence of a weak network structure, exhibiting thixotropic behavior, has been shown, down to reduced concentrations C[η] much lower than that corresponding to coil overlap. Maximum synergistic effects are observed for a xanthan/carob (X/C) ratio of 5·5/4·5. The formation of the network is dependent on the aging time, and, for very dilute systems, a very low shear rate is necessary to observe a transitory network. From viscosity measurements after disruption of the structure under shear, the intrinsic viscosity and the apparent Huggins coefficient of several X/C mixtures have been determined. They show a decrease in the average hydrodynamic volume of the polymers and a high tendency to aggregation at X/C ratios corresponding to network formation. To take into account all the observed phenomena, a mechanism involving the formation of stable aggregates and of shear-sensitive 'superaggregates' is proposed.*

INTRODUCTION

Xanthan and carob gums are thickeners which form a thermoreversible gel on mixing. These synergistic effects have been known for a long time and have more and more technological applications, particularly in the food industry (Rocks, 1971; Kovacs, 1973).

The extracellular microbial polysaccharide xanthan has a pentasaccharide repeat unit formed by a $\beta(1-4)$-linked D-glucose backbone, as in cellulose, C-3 substituted by a charged trisaccharide side-chain (Jansson *et al.*, 1975).

A review of the production, properties and applications of this biopolymer has been recently published by Kennedy & Bradshaw (1984).

Carbohydrate Polymers 0144-8617/88/$03.50 —

In aqueous solution at a sufficiently high ionic strength, the macromolecule is in an ordered state (Morris *et al.*, 1977; Holzwarth, 1978; Rinaudo & Milas, 1978; Milas & Rinaudo, 1979; Norton *et al.*, 1980; Paoletti *et al.*, 1983). This conformation seems to be dependent on the thermal history of the sample (Milas & Rinaudo, 1984; Milas *et al.*, 1986). A rigid rod or a semi-rigid wormlike model is commonly used to explain the large low-shear-rate viscosity and the pronounced shear thinning behavior of aqueous xanthan solutions (Whitcomb & Macosko, 1978; Holzwarth, 1981; Chauveteau, 1982; Paradossi & Brant, 1982; Ross-Murphy *et al.*, 1983; Muller *et al.*, 1984). The influence of concentration on the viscous and viscoelastic properties of xanthan solutions has been recently described (Cuvelier and Launay, 1986*a*), and a hypothesis of self association in the semi-dilute domain, consistent with the conclusions of other workers (Southwick *et al.*, 1980, 1981, 1982; Frangou *et al.*, 1982; Morris *et al.*, 1983; Jamieson *et al.*, 1983), has been proposed.

Carob gum is a plant seed (*Ceratonia siliqua*) galactomannan; its chemical structure is based on a $\beta(1-4)$ linked mannan backbone C6-substituted by α-galactosyl residues. In aqueous solution, this neutral macromolecule adopts a rather extended random coil conformation (Sabater de Sabates, 1979).

The average degree of substitution is about 1/4, but the distribution of galactose along the mannan chain is irregular, with unsubstituted and completely substituted regions. This block structure has been assumed to be responsible for gelling interactions with xanthan or carrageenan (Dea and Morrisson, 1975; Dea *et al.*, 1977; Morris *et al.*, 1980) because specific interactions occur between the helical polysaccharide chains and the 'smooth' regions of the carob chain.

Investigations have been performed recently on different natural or enzymatically debranched galactomannans, in order to understand their interaction with other polysaccharides better and particularly the influence of the distribution of galactose along the chain (McCleary, 1979; McCleary *et al.*, 1981; McCleary *et al.*, 1984; Cheetham *et al.*, 1986; Clark *et al.*, 1986; Dea *et al.*, 1986). The major role of the totally unsubstituted mannan regions of the backbone has been well established (McCleary *et al.*, 1984; Dea *et al.*, 1986). For the galactomannans having insufficiently long unsubstituted regions, interactions with other polysaccharides may involve sections of galactomannan where galactosyl groups are positioned only on one side of the D-mannan backbone (McCleary, 1979; Dea *et al.*, 1986).

The model of interchain binding between the unsubstituted regions of the carob galactomannan and xanthan helices is still under discussion.

Recently, from X-ray fiber diffraction patterns, Cairns *et al.* (1986), have suggested the possibility of a 'sandwich' structure involving an unsubstituted mannan backbone between two xanthan chains. Tako *et al.* (1984) have reported stronger interactions with deacetylated than with native xanthan molecule, and they have proposed an intermolecular mechanism involving the side chains of the xanthan.

Preliminary results have been reported on the viscoelastic properties of xanthan–carob mixed gels (Cuvelier & Launay, 1986*b*). Dynamic measurements have been performed in the semi-dilute domain (total concentration 0·5 g dl^{-1}) at different xanthan/carob ratios. Maximum synergistic effects have been observed for a system containing about 70% xanthan. An aging time effect has also been described and xanthan/xanthan interactions have been assumed to play a part in the viscoelastic properties of the gel. The present study aims to investigate more completely xanthan–carob interactions at very low concentrations using viscosity measurements.

MATERIALS AND METHODS

Xanthan gum (X) was a commercial food grade sample (Rhodigel 23, Na form, degree of pyruvylation 1/3, acetate 100%) kindly supplied by Rhône-Poulenc (France), and carob (C), a purified sample, 'Rein Karubin' (mannose/galactose ratio = 2·8), kindly supplied by Meyhall Chemical (Switzerland). Intrinsic viscosity of these samples in 0·1 M NaCl aqueous solvent has been determined at 25°C to be 48·5 and 12·8 dl g^{-1} for xanthan and carob respectively.

Solutions of each polymer were prepared at a concentration of 0·6 g dl^{-1} (dry basis) by dispersing the gum in 0·1 M NaCl, with 0·05% NaN_3 as antimicrobial agent, stirring at room temperature for 30 min, then at 80°C for 1 h.

X/C preparations at 0·6 g dl^{-1} containing various amounts of X and C were made by mixing for 30 min at 80°C the required volumes of each solution, and diluting with 0·1 M NaCl.

Before each measurement, the final X/C mixtures were stirred for 15 min at 70°C, and then put in the viscometer and thermostated at 25°C for the required time.

The viscometer was a Low Shear 30 (Contraves, Zurich) equipped with coaxial cylinders (radius ratio 0·92), with a Rheoscan 30 programmer for automatically registering flow curves and shear stress-time curves.

RESULTS

Nine X/C preparations have been studied at different ratios from 1/9 to 9/1. All the 0·6 g dl^{-1} mixtures gave 'sensible gels' at room temperature, and shear thinning solutions at 70°C.

At 25°C, viscosity measurements were feasible with sufficiently dilute mixtures, and, in such a case, we have systematically registered the flow curves of more and more dilute systems, after 15 min aging time in the viscometer. Three typical flow curves obtained for the X/C ratio = 6/4

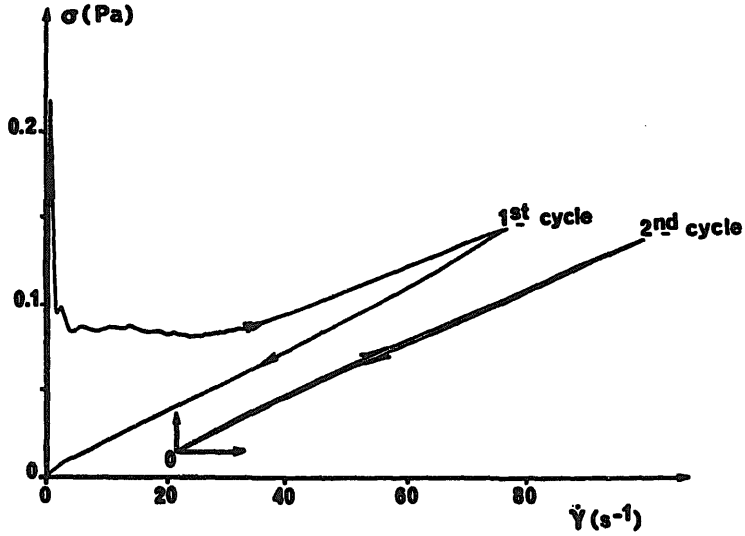

Fig. 1(a). Flow curve of xanthan/carob mixture at a total concentration of 0·01 g dl^{-1}, X/C = 6/4, 25°C. First cycle after 15 min aging time, second cycle after a shearing time of 3 min at 70 s^{-1}. Run time cycle: 4 min.

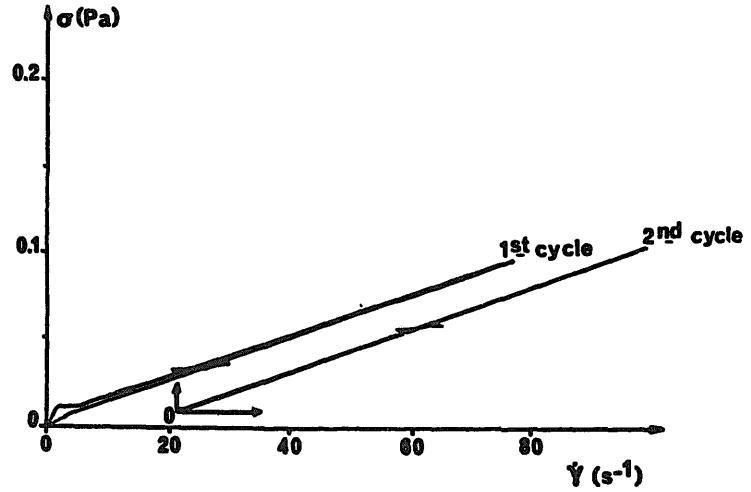

Fig. 1(b). As Fig. 1(a), total concentration: 0·007 g dl^{-1}.

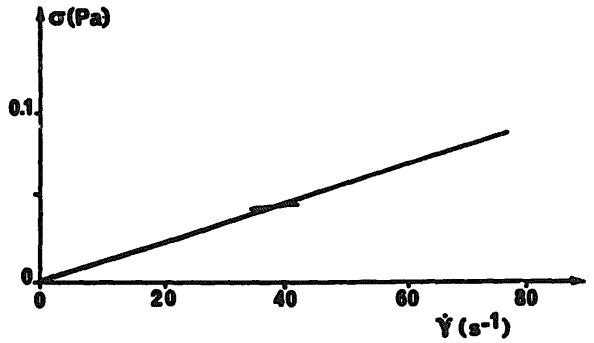

Fig. 1(c). As Fig. 1(a), total concentration: 0·005 g dl^{-1}. Successive shearing cycles give superimposed curves.

are reproduced in Figs 1(a), 1(b) and 1(c); a very marked thixotropic behavior is observed at a total concentration of 0·01 g dl^{-1} (Fig. 1(a)), due to the formation of a weak gel structure which is very shear sensitive; after shearing for 3 min at 70 s^{-1}, the structure has been broken down, and a second cycle exhibits just a small gap between the up and down flow curves. On decreasing the total concentration, to 0·007 g dl^{-1}, a structural breakdown is still apparent on the first cycle, but after shearing, thixotropic effects are no longer observed (Fig. 1(b)). At 0·005 dl g^{-1}, the solution showed Newtonian behavior from the first cycle (Fig. 1(c)).

The behavior under shearing of the weak gel obtained under the previous conditions (X/C ratio = 6/4, 0·007 g dl^{-1}), has been studied by applying a constant low shear rate (0·47 s^{-1}) and registering the shear stress (Fig. 2). The immediate stress peak observed is characteristic of the weak gel structure, which is then destroyed under shearing, bringing about a stress decrease until an equilibrium value has been reached. It has also been observed that the equilibrium stress is reached after longer times under lower shear rates. After a few seconds stopping, restarting at the same shear rate gives immediately the same shear stress: therefore, the initial peak is not due to a stress-overshoot phenomenon. If more severe shearing is carried out (70 s^{-1}, 3 min), the structure is more disrupted than before as shown bv shearing again at the same low shear rate; but, a time-dependent restructuring is observed, leading to the same equilibrium state.

The restructuring mechanism is also effective at rest: after 2 hours, an initial peak is observed again, but this is smaller than the first one. This can be explained by the effect of the rest time at 25°C which would be less efficient than cooling from 70°C to 25°C for the building of the network.

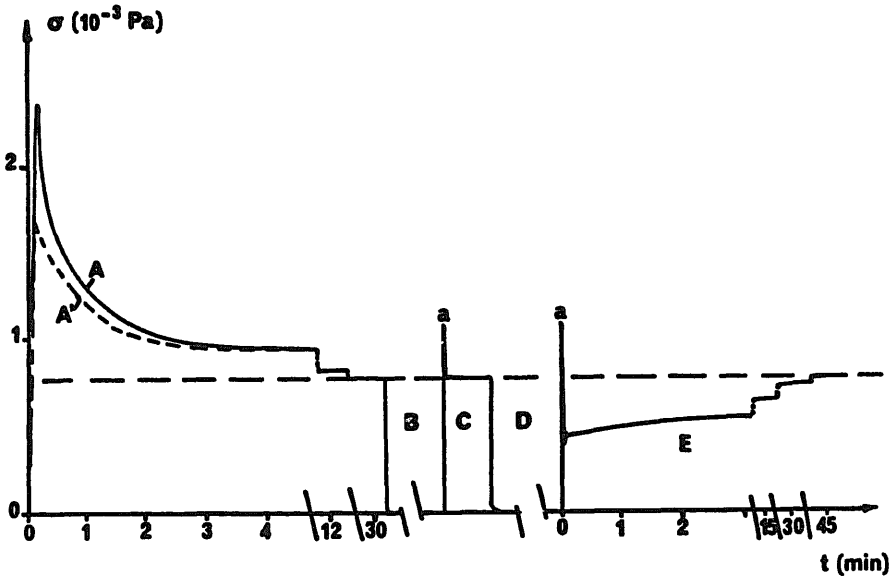

Fig. 2. Shear stress as a function of time at 0·47 s^{-1}. Total concentration: 0·007 g dl^{-1}, X/C = 6/4, 25°C. A, first shearing after 15 min. aging time; B, stop and C, immediate restarting; D, 5 min. shearing at 70 s^{-1} and then E, shearing at 0·47 s^{-1}; A', shearing at 0·47 s^{-1} after 2 hours recovery. The very sharp peak (a) registered when shearing begins is due to inertial effects.

For all mixtures at concentrations giving a Newtonian behavior after 15 min at 25°C, we have extended the aging time in the viscometer (Fig. 3). At low shear rate (0·95 s^{-1}), two phenomena were then displayed; (i) beyond a critical aging time, a stress peak due to a network structure is observed but the maximum of the peak is not immediately observed (it corresponds to a strain value of about 80), implying a shear effect to build up the structure; (ii) the longer the aging time, the higher the stress peak, indicating a more and more organized structure.

In Fig.4, we have summarized on a phase diagram all the qualitative observations obtained for the mixtures at different X/C ratios, using three arbitrary criteria:

- G: mixtures having marked gel properties after 15 min aging (Fig. 1(a));
- T: mixtures having a weak thixotropic behavior under the same measurement conditions (Fig. 1(b));
- P: mixtures for which a stress peak is observed at low shear rate (0·95 s^{-1}) after 2 hours aging-time (Fig. 3).

The most effective interactions between the two polymers are obtained for X/C ratios between 5/5 and 7/3. Because of the influence of

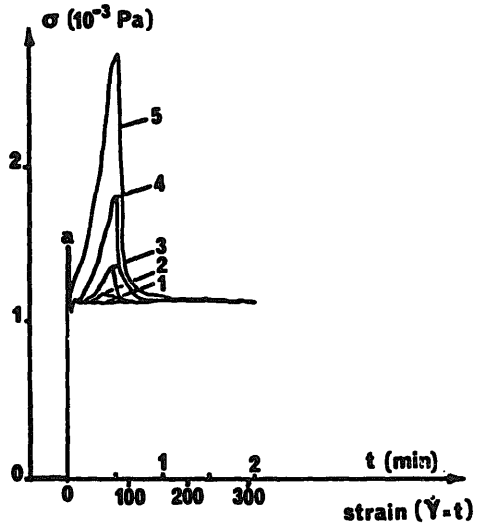

Fig. 3. Shear stress as a function of time at 0·95 s^{-1}. Total concentration: 0·005 g dl^{-1}, X/C = 6/4; aging time at 25°C: 1, 15 min; 2, 30 min; 3, 1 hour; 4, 2 hours; 5, 3 hours; (a), see Fig. 2.

aging time on the structuring of the medium, we have to consider that there is no discontinuity between the domains depicted on Fig. 4, and curve P could have been lowered if longer aging times had been used. In any event whatever the selected criterion, it is apparent that the shapes of the boundary curves are approximately the same: the minimum concentration at which noticeable interaction effects are obtained is at similar X/C ratios (5/5 to 7/3).

It is noteworthy that the gel–sol limits in the phase diagram are much lower than the one deduced from $C[\eta] = 1$, a value of the 'overlap parameter' which could imply full occupancy of available space by polymer coils (Launay *et al.*, 1986). The same conclusion is reached, whether taking $[\eta]$ as the ratio average intrinsic viscosity of xanthan and of carob alone, or using the one calculated from experimental measurements (see Figs 6 and 7).

The Newtonian behavior after shearing of the diluted mixtures (Fig. 1) has been confirmed by stepwise measurements at shear rates from 70 to 1·7 s^{-1}. At very low concentrations, a constant value of η is obtained over the whole of this range. For more concentrated solutions, on decreasing the shear rate, one can observe an increase in apparent viscosity with shearing time as described above (Fig. 2). At a given low shear rate, there is an equilibrium state corresponding to a more aggregated system reached after rather long times. The values obtained at 70 s^{-1}, where viscosity becomes independent of shear rate, have been

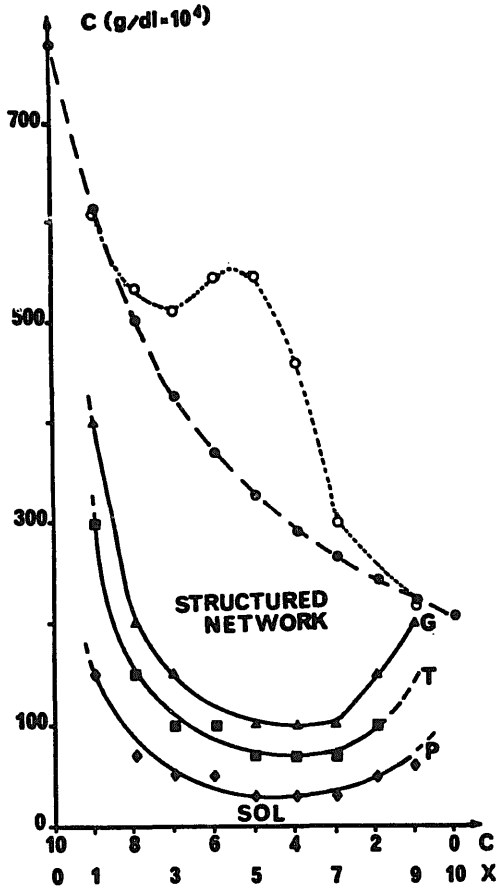

Fig. 4. Phase diagram for mixtures at different X/C ratios. See text for criteria G, T and P. ●, concentration corresponding to $C[\eta]=1$ with $[\eta]=[\eta]_{calc}$ calculated with eqn. (2), or: ○, with $[\eta]=[\eta]_M$ deducted from experimental results (eqn. (1)).

used in these cases (see Figs 5 and 6).

Figure 5 shows the relationship between viscosity and X/C ratio at four concentrations: synergistic effects increasing with concentration are obvious from concentrations of 0·005 g dl^{-1}, and a maximum is observed for X/C ratio = 6/4.

These values were used to estimate the intrinsic viscosity $[\eta]_M$ and an apparent Huggins coefficient λ_M, at a given X/C ratio (Fig. 6):

$$(\eta_{sp}/C)_M=[\eta]_M+\lambda_M[\eta_M]^2C \qquad (1)$$

η_{sp} is the specific viscosity of the concentration C. It can be observed in Figs 5 and 6 that the values corresponding to systems which are disaggregated by shearing are consistent with those for which a Newtonian behavior has been registered (Fig. 1(c)) without shearing time effects.

If there were no specific interchain associations between xanthan and carob, and no purely thermodynamical effects of mixing, we should

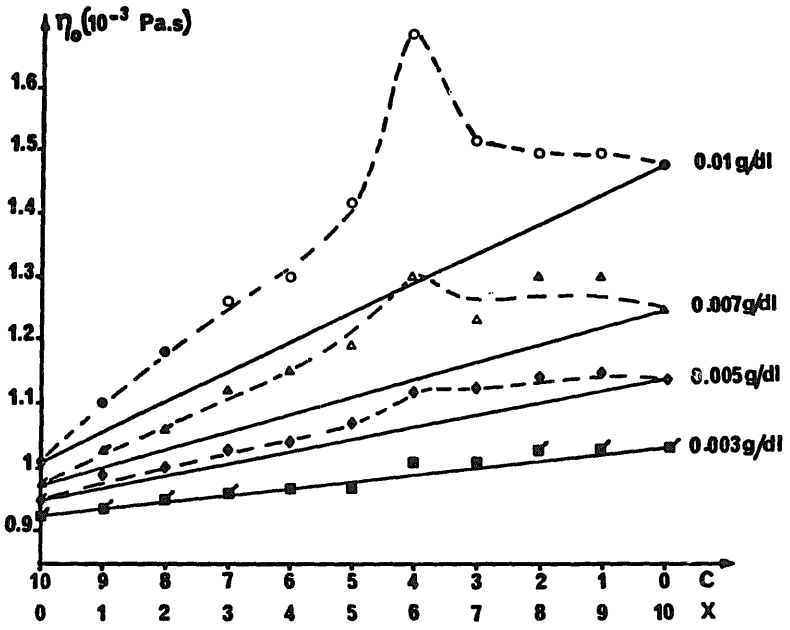

Fig. 5. Viscosity of 4 mixtures as a function of different X/C ratios. ■◆▲●, Newtonian viscosity; △○, viscosity at 70 s^{-1} after disaggregation under shear (see text); ■◆▲, calculated values from experimental results and eqn. (1).

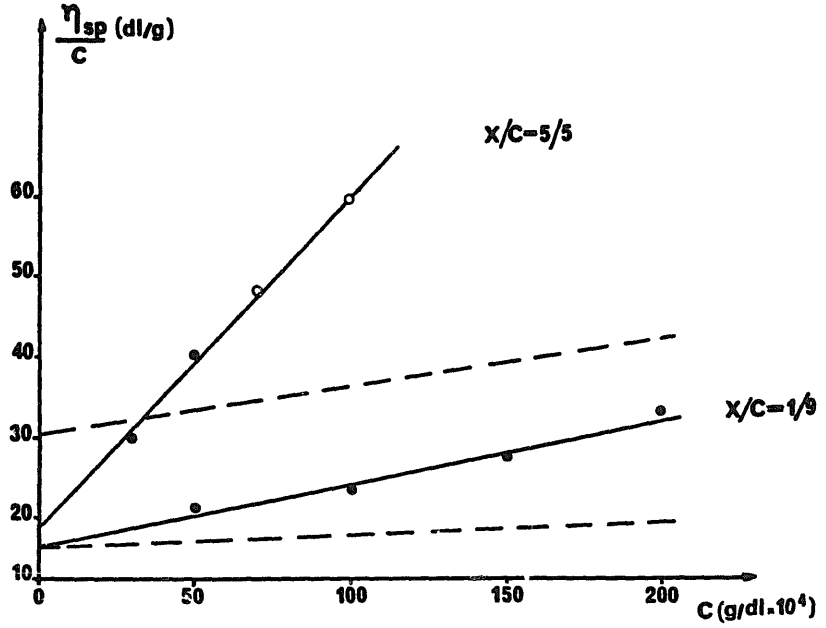

Fig. 6. Reduced specific viscosity as a function of concentration at two X/C ratios at 25°C; ●, Newtonian viscosity; ○, viscosity at 70 s^{-1} after disaggregation under shear (see text); dotted lines calculated with eqn. (2).

expect only additivity of hydrodynamic volumes and additivity of hydrodynamic interactions between isolated chains. This would lead to a theoretical variation of the reduced specific viscosity, $(\eta_{sp}/C)_{calc}$, calculated from intrinsic viscosities ($[\eta]_X$, $[\eta]_C$) and Huggins coefficients (λ_X, λ_C), determined for the two polymers alone in the same solvent, given by eqn. (2):

$$(\eta_{sp}/C)_{calc} = [\eta]_{calc} + \lambda_{calc}[\eta_{calc}]^2 C \qquad (2)$$

with

$$[\eta]_{calc} = A[\eta]_X + (1-A)[\eta]_C$$

$$\lambda_{calc} = A\lambda_X + (1-A)\lambda_C$$

$A/(1-A)$: value of X/C ratio

Figure 6 shows the comparison between experimental results and the values calculated with eqn. (2) at two X/C ratios (5/5 and 1/9). When a component is predominant in the mixture (X/C = 1/9), the intrinsic viscosity corresponds approximately to the average value calculated with eqn. (2). The increase of reduced specific viscosity, η_{sp}/C, with concentration is due to a value of λ_M which is much greater than the one calculated, (λ_{calc}), from eqn. (2). For more synergistic ratios (for example X/C = 5/5, Fig. 6), the situation is very different: the experimental intrinsic viscosity is much lower than the calculated one. This effect is dominant at very low concentrations leading to a lower value of η_{sp} compared to the one calculated with eqn. (2); however, at a sufficiently high concentration, the very high value of λ_M is dominant and η_{sp} is higher.

Figures 7 and 8 summarize the results obtained for all studied X/C ratios, compared with the expected values if only additive hydrodynamic effects occurred.

Figure 8 shows clearly that the most important reduction of intrinsic viscosity ($\Delta[\eta] = [\eta]_M - [\eta]_{calc}$) and the maximum value of $\Delta\lambda = \lambda_M - \lambda_{calc}$, indicating maximum tendency to aggregation, are observed for the same X/C ratio of 5·5/4·5.

Xanthan/carob interactions at low concentration lead to two opposite effects:

- a diminution of the average hydrodynamic volume at infinite dilution;
- an aggregation phenomenon when concentration increases.

The latter effect is dominant on the variation of viscosity from very low concentrations, leading to the synergistic effect described in Fig. 5 for 0·005 g dl^{-1} and above.

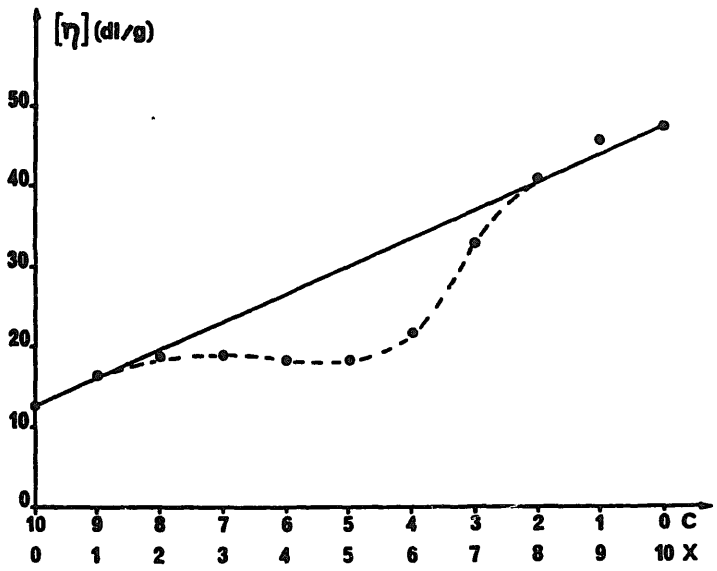

Fig. 7. Intrinsic viscosity as a function of X/C ratio (eqn. (1)).

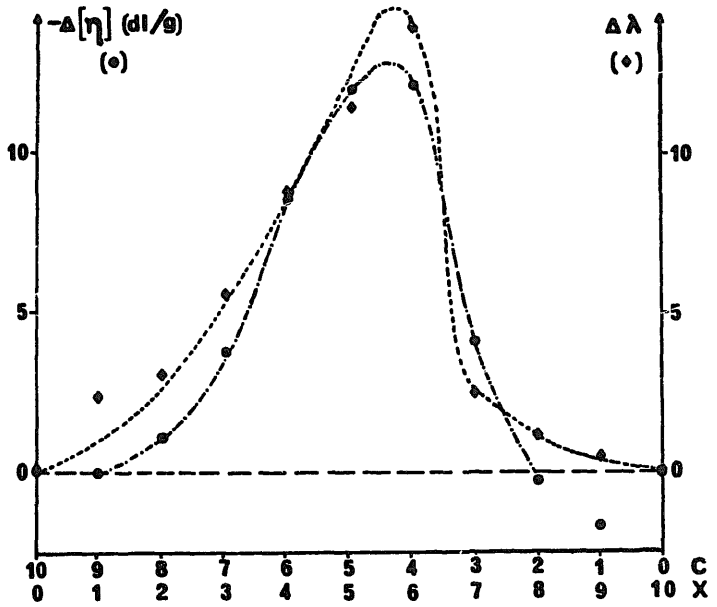

Fig. 8. Synergistic effects: variation of $\Delta\lambda$ and $-\Delta[\eta]$ as a function of X/C ratio.

It is to be noted that Privalov *et al.* (1971) have also demonstrated the formation of a weak elastic network in dilute tropocollagen solutions under low shear conditions. However, this effect is observed over an optimum concentration range, in contrast to our own results. Therefore, the proposed mechanism, based on a hypothetical liquid crystal organization of the macromolecules, cannot be retained here.

CONCLUSION

The results presented here demonstrate, in mixed xanthan/carob systems at very low reduced concentrations ($C[\eta] << 1$), the existence of a weak gel structure which is shear rate dependent. Newtonian behavior observed after a shearing period is consistent with an hypothesis of a stable state of aggregation at given total concentration and X/C ratio.

The structuring of the medium during aging involves the formation of 'superaggregates' leading to network formation at rest if the concentration is sufficient and the aging time long enough. At very low concentrations the application of a low shear rate results in network formation. We suggest that slow shearing could organize the 'superaggregates' into a weak transitory network. This mechanism could be analogous to orthokinetic flocculation.

The following schema sums up our main conclusions:

Formation of X–C elementary units brings about a decrease in hydrodynamic volume. This association process, presented here as the first step in the structuring of the medium, is consistent with the existence of specific interactions between xanthan chains and smooth regions of carob proposed by numerous workers as cited in the Introduction. In agreement with these previous studies, we assume that a strong interchain affinity is more realistic than a mechanism based purely on thermodynamical incompatibility.

These units have a very pronounced self affinity, leading to progressive aggregation when the concentration increases, as shown by the anomalously high values of the apparent Huggins coefficient λ_M. The thermoreversibility of these phenomena observed by heating the medium at 70°C means that interactions at any level are reversible. Maximum synergistic effects occur at a xanthan/carob ratio = 5·5/4·5 for the samples studied. Whatever the concentrations in the dilute domain, the stoichiometry corresponds to this ratio. If a xanthan molecular weight of 2×10^6 is assumed (Launay *et al.*, 1985), and about 10^6 for carob (Sabater de Sabates, 1979), the relative composition of the elementary X/C units should be 2 to 3 carob chains to 1 xanthan chain, taking into account the presence of a completely branched fraction in the carob sample (Sabater de Sabates, 1979).

At higher reduced concentrations ($C[\eta] > 1$), corresponding to the formation of firm gels, additional mechanisms such as xanthan–xanthan interactions (Cuvelier & Launay, 1986*a*) are probably implied due to the high occupancy of the medium by macromolecular chains. It probably explains why the same samples gave an optimum X/C ratio of 7/3 in the semi-dilute domain (Cuvelier & Launay, 1986*b*).

From a technological viewpoint, the properties described here could explain the efficiency of xanthan/carob mixtures at very low concentrations as a suspending or stabilizing agent in liquid foodstuffs.

REFERENCES

Cairns, P., Miles, M. J. & Morris, V. J. (1986). *Nature*, **322**, 89.

Chauveteau, G. (1982). *J. Rheology*, **26**, 111.

Cheetham, N. W. H., McCleary, B. V., Tang, G., Lum, F. & Maryanto. (1986). *Carbohydr. Polym.*, **6**, 257.

Clark, A. H., Dea, I. C. M. & McCleary, B. V. (1986). In: *Gums and Stabilisers for the Food Industry*, Vol. 3, eds. Phillips, G. O., Wedlock, D. J. & Williams, P. A., Elsevier Applied Science, London, p. 429.

Cuvelier, G. & Launay, B. (1986*a*). *Carbohydr. Polym.*, **6**, 321.

Cuvelier, G. & Launay, B. (1986*b*). In: *Gums and Stabilisers for the Food Industry*, Vol. 3, eds. Phillips, G. O., Wedlock, D. J. & Williams, P. A., Elsevier Applied Science, London, p. 147.

Dea, I. C. M., Clark, A. H. & McCleary, B. V. (1986). *Food Hydrocolloids*, **1**, 129.

Dea, I. C. M., Morris, E. R., Rees, D. A., Welsh, E. J., Barnes, M. A. & Price, J. (1977). *Carbohydr. Res.*, **57**, 249.

Dea, I. C. M. & Morrisson, A. (1975). *Adv. Carbohydr. Chem. Biochem.*, **31**, 241.

Frangou, S. A., Morris, E. R., Rees, D. A., Richardson, R. K. & Ross-Murphy, S. B. (1982). *J. Polym. Sci., Polym. Letters Ed.*, **20**, 531.

Holzwarth, G. (1978). *Carbohydr. Res.*, **66**, 173.

Holzwarth, G. (1981). *Am. Chem. Soc. Symp. Ser.*, **150**, 15.

Jamieson, A. M., Southwick, J. G. & Blackwell, J. (1983). *Faraday Symp. Chem. Soc.*, **18**, 131.

Jansson, P. E., Kenne, L. & Lindberg, B. (1975). *Carbohydr. Res.*, **45**, 275.

Kennedy, J. F. & Bradshaw, I. J. (1984). *Prog. Ind. Microbiol.*, **19**, 319.

Kovacs, P. (1973). *Food Technol.*, **27**, 26.

Launay, B., Cuvelier, G. & Martinez-Reyes, S. (1985). In: *Gums and Stabilisers for the Food Industry*, Vol. 2, eds. Phillips, G. O., Wedlock, D. J. & Williams, P. A., Pergamon Press, Oxford, p. 79.

Launay, B., Doublier, J. L. & Cuvelier, G. (1986) In: *Functional Properties of Food Macromolecules*, eds. Mitchell, J. R. and Ledward, D. A. Elsevier Applied Science, London, p. 1.

McCleary, B. V. (1979). *Carbohydr. Res.*, **71**, 205.

McCleary, B. V., Amado, R., Waibel, R. & Neukom, M. (1981). *Carbohydr. Res.* **92**, 269.

McCleary, B. V., Dea, I. C. M., Windust, J. & Cooke, D. (1984). *Carbohydr. Polym.*, **4**, 253.
Milas, M. & Rinaudo, M. (1979). *Carbohydr. Res.*, **76**, 189.
Milas, M. & Rinaudo, M. (1984). *Polym. Bull.*, **12**, 507.
Milas, M. & Rinaudo, M. & Tinland, B. (1986). In *Gums and Stabilisers for the Food Industry*, Vol. 3, eds. Phillips, G. O., Wedlock, D. J. & Williams, P. A. Elsevier Applied Science, London, p. 637.
Morris, E. R., Rees, D. A., Young, G., Walkinshaw, M. D. & Darke, A. (1977). *J. Mol. Biol.*, **110**, 1.
Morris, E. R., Rees, D. A., Robinson, G. & Young, G. A. (1980). *J. Mol. Biol.* **138**, 363.
Morris, V. J., Franklin, D. & l'Anson, K. (1983). *Carbohyd. Res.*, **121**, 13.
Muller, G., Lecourtier, J., Chauveteau, G. & Allain, C. (1984). *Makromol. Chem., Rapid. Commun.*, **5**, 203.
Norton, I. T., Goodall, D. M., Morris, E. R. & Rees, D. A. (1980). *J. Chem. Soc. Chem. Commun.*, 545.
Paoletti, S., Cesaro, A. & Delben, F. (1983). *Carbohydr. Res.*, **123**, 173.
Paradossi, G. & Brant, D. A. (1982). *Macromolecules*, **15**, 874.
Privalov, P. L., Serdyuk, I. N. & Tiktopulo, E. I. (1971). *Biopolymers*, **10**, 1777.
Rinaudo, M. & Milas, M. (1978) *Biopolymers*, **17**, 2663.
Rocks, J. K. (1971). *Food Technol.*, **25**, 476.
Ross-Murphy, S. B., Morris, V. J. & Morris, E. R. (1983). *Faraday Symp. Chem. Soc.*, **18**, 115.
Sabater de Sabates, A. (1979). Contribution à l'étude des relations entre caractéristiques macromoléculaires et propriétés rhéologiques en solution aqueuse concentrée d'un épaississant alimentaire: la gomme de caroube. Thèse de Doctorat-Ingénieur — ENSIA — Universités Paris VII et Paris XI.
Southwick, J. G., Lee, H., Jamieson, A. M. & Blackwell, J. (1980). *Carbohydr. Res.*, **84**, 287.
Southwick, J. G., Jamieson, A. M. & Blackwell, J. (1981). *Macromolecules*, **14**, 1728.
Southwick, J. G., Jamieson, A. M. & Blackwell, J. (1982).*Carbohydr. Res.*, **99**, 117.
Tako, M., Asato, A. & Nakamura, S. (1984). *Agric. Biol. Chem.*, **48**, 2995.
Whitcomb, P. J. & Macosko, W. (1978). *J. Rheology*, **22**, 493.